

# Coulomb Explosion: A Novel Approach to Separate Single-Walled Carbon Nanotubes from Their Bundle

Guangtong Liu,<sup>†,‡</sup> Yuanchun Zhao,<sup>†,§</sup> Kaihong Zheng,<sup>†,§</sup> Zheng Liu,<sup>†,§</sup>  
Wenjun Ma,<sup>‡,§</sup> Yan Ren,<sup>‡,§</sup> Sishen Xie,<sup>\*,‡</sup> and Lianfeng Sun<sup>\*,†</sup>

National Center for Nanoscience and Technology, Beijing 100190, China, Beijing  
National Laboratory for Condensed Matter Physics, Institute of Physics, Beijing  
100190, China, and Graduate School of Chinese Academy of Sciences,  
Beijing 100049, China

Received September 17, 2008; Revised Manuscript Received November 23, 2008

## ABSTRACT

A novel approach based on Coulomb explosion has been developed to separate single-walled carbon nanotubes (SWNTs) from their bundle. With this technique, we can readily separate a bundle of SWNTs into smaller bundles with uniform diameter as well as some individual SWNTs. The separated SWNTs have a typical length of several microns and form a nanotree at one end of the original bundle. More importantly, this separating procedure involves no surfactant and includes only one-step physical process. The separation method offers great conveniences for the subsequent individual SWNT or multiterminal SWNTs device fabrication and their physical properties studies.

Single-walled carbon nanotubes (SWNTs) have received intensified interest due to their unique structures and properties since their discovery.<sup>1</sup> Theoretical calculations predicted that SWNTs can be metallic or semiconducting depending on their diameters and helicity,<sup>2,3</sup> and these predictions have been confirmed by scanning tunneling microscope (STM) studies.<sup>4,5</sup> However, the as-grown SWNTs synthesized by conventional methods are often tangled with each other and readily form bundles with a large van der Waals binding energy ( $\sim 500$  eV per microns of tube–tube contact).<sup>6,7</sup> This bundling modifies the electronic structure of carbon nanotubes<sup>8</sup> and confounds all attempts to separate the nanotubes according to size or type. This has been a major obstacle for potential applications of SWNTs in nanodevices and nanoelectronic circuits. To overcome this limitation, many researchers have explored selective chemistry to obtain monodispersed SWNTs. Following selective chemical functionalization, individual SWNTs are then separated from their bundles<sup>9–11</sup> using a variety of techniques including electrophoretic separation<sup>12,13</sup> and/or chromatographic methods.<sup>14–17</sup> However, these chemical routes based on solution-phase involve not only polymer or surfactants, but also multistep

chemical and physical processes. In the meantime, these chemical approaches have doping effects on SWNTs,<sup>18–20</sup> which modifies the properties of the SWNTs. Moreover, the obtained individual SWNTs are usually very short (ranging from several tens to hundreds of nanometers) and tend to aggregate in solutions. These drawbacks displayed in the above chemical separation methods limit the fabrication and property studies of SWNTs devices. It is necessary to explore new methods that can separate nanotubes from their bundles by simple physical means, which should be performed directly on the substrates and thus avoiding chemical modifications.

Here we demonstrate that a novel effect of Coulomb charging can be employed to separate SWNTs. The Coulomb effect exists ubiquitously in physics, chemistry, and biology. A well-known manifestation of this effect is Coulomb explosion observed in stability of a cluster. It is defined classically by Rayleigh instability limit,<sup>21</sup> above which an excessively charged cluster becomes unstable and explodes into smaller fragments. This method has been used for controlled fabrication of metal nanostructures recently.<sup>22</sup> In this letter, we demonstrate a novel method to separate SWNTs from a SWNT bundle by using Coulomb explosion. With this technique, we can readily separate a bundle of SWNTs into smaller bundles with uniform diameter as well as some individual SWNTs. The separated SWNTs have a typical length of several microns and form a nanotree at one

\* To whom correspondence should be addressed. E-mail: (L.F.S.) slf@nanoctr.cn; (S.S.X.) sxxie@aphy.iphy.ac.cn. Telephone: 86-10-82545584. Fax: 86-10-62656765.

<sup>†</sup> National Center for Nanoscience and Technology.

<sup>‡</sup> Institute of Physics.

<sup>§</sup> Graduate School of Chinese Academy of Sciences.

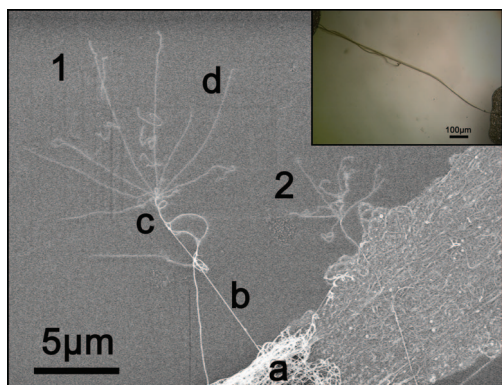


**Figure 1.** SEM image of two typical nanotrees of SWNTs formed at the ends of two SWNT bundles via Coulomb explosion. These two nanotrees are almost perpendicular to the SWNT rope. The inset shows the optical image of the device (scale bar: 100  $\mu\text{m}$ ).

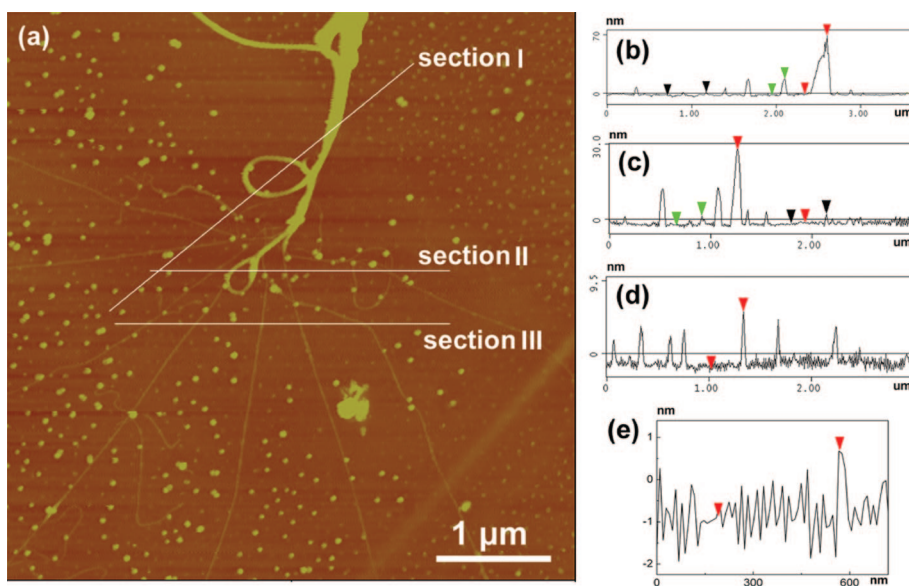
end of the original bundle. Compared to the existing chemical separation methods, this separating procedure has at least three advantages. First, it is a physical separation method and involves no surfactant. Therefore, the doping effects caused by these chemicals can be avoided,<sup>18–20</sup> which may convert semiconducting SWNT to metallic one, or vice versa. Second, it can be done on different substrates, such as silicon and sapphire, which provide great conveniences for the individual SWNT device or multiterminal SWNTs device fabrication.<sup>23</sup> Third, it involves only one-step process and can be realized easily. These advantages make this separation method promising for the nanodevice fabrication and physical property studies.

SWNTs used in this study were synthesized by floating catalytic chemical vapor deposition (CVD).<sup>24,25</sup> In order to make the SWNTs charged, we fabricated a two-terminal device in the following process. First, a SWNT rope was transferred onto a glass slide with a tweezers. Then, two silver paint drops were placed on it, which were connected

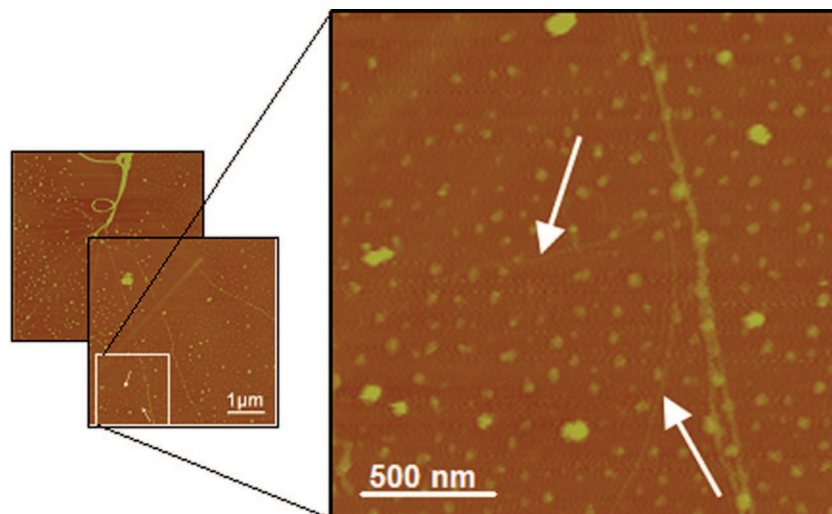
to two platinum wires serving as source and drain electrodes, respectively (Figure 1, inset). The typical SWNT rope used in our experiment has a diameter of  $\sim 10 \mu\text{m}$  and a length of  $\sim 1.1 \text{ mm}$ . The 2-probe resistance of the device is several thousands Ohm at room temperature. Keithley 4200 was employed as the constant voltage source. During charge process, one electrode was connected to the constant voltage source, while the other electrode is floated.

Figure 1 shows a typical scanning electron microscopy (SEM) image of the SWNT rope, SWNT bundles, as well as the separated SWNTs after charging about 50 s with an electrostatic potential about 15 V. From this image, three distinct characteristics of these separated SWNTs can be found. First, the separation of SWNTs mainly occurred at one end of a SWNT bundle, which is almost perpendicular to the SWNT rope. Second, all these separated SWNTs radiate from one center, such as that denoted by c in “nanotree 1”. Third, these isolated SWNTs are relatively straight and separated from each other as far as possible. These features are very similar to the case of branches stretching from a tree. Therefore, we call this novel structure “nanotree”.

The structures of the nanotree 1 are further studied with an atomic force microscopy (AFM, Digital Instruments Nanoscope IIIA) operating in the tapping mode (Figure 2). It can be seen that all the separated SWNTs extend from one point of the SWNT bundle. The corresponding section analyses of the AFM image at sections “I”, “II”, and “III” are shown in Figure 2b–d, respectively. The height of SWNTs is 69.6, 19.3, and 3.3 nm for section I; 29.1, 4.3, and 3.7 nm for section II; and 7.6, 4.3, and 2.7 nm for section III, respectively. Therefore, these separated branches ( $\sim 3 \text{ nm}$ ) of SWNT nanotree consists of 3~6 individual SWNTs. If we inspect the AFM image carefully, it is not difficult to find that there are some individual separated SWNTs. Figure 3 shows two individual SWNTs (indicated by the white arrows) at the terminals of the SWNT nanotree. The



**Figure 2.** (a) AFM image of the nanotree 1 of SWNTs formed at one end of the SWNT bundle. (b–d) Height analyses at sections I, II, and III. (e) An individual SWNT with a diameter of  $\sim 1.5 \text{ nm}$ .



**Figure 3.** Individual SWNTs (indicated by the white arrows) at the terminals of the SWNT nanotree. The corresponding section analysis is shown in Figure 2e.

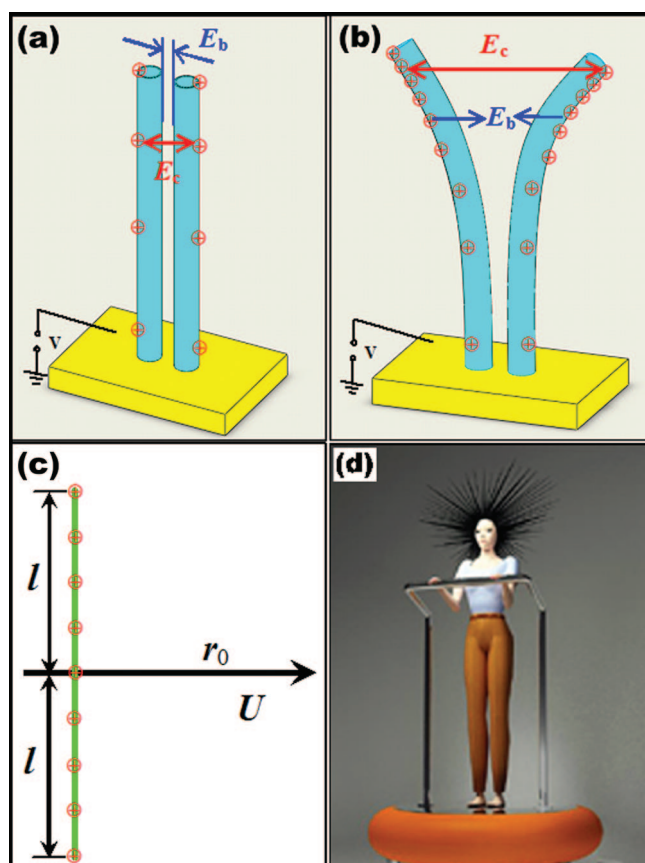


**Figure 4.** Schematic illustration of a typical separation process for a SWNT bundle. (a) The SWNT bundle before Rayleigh instability limit is reached. (b) The SWNT bundle after Coulomb explosion. (c) The potential at a distance  $r_0$  produced by linear distribution of charges. (d) A cartoon showing the hairs separating from each other and extending radially from the head because of charging.

corresponding section analysis shown in Figure 2e indicates that the diameter of the separated SWNT is  $\sim 1.5$  nm, which demonstrates that the separated SWNTs are indeed individual SWNT.

In 1882, Lord Rayleigh<sup>21</sup> studied the stability of the charged droplets theoretically. For an incompressible charged liquid droplet, he found that the quadrupole oscillation becomes unstable when the disruptive Coulomb force is equal to the attractive cohesive force. This is the famous Rayleigh instability limit. If this condition is satisfied, the repulsive Coulomb energy ( $E_c$ ) will be twice as much as the cohesive surface energy ( $E_s$ )<sup>26</sup>

$$E_c = 2E_s \quad (1)$$

Comparing our experimental observations with the classical charged droplet, quite similar features can be found. Therefore, we propose that the underlying mechanism for the separation of SWNTs in a bundle is Coulomb explosion, which is further analyzed in the following.

For simplicity, we consider two individual SWNTs as shown in Figure 4. Before they are charged, due to van der Waals binding energy, these SWNTs are linked to each other with a spacing of  $\sim 0.34$  nm.<sup>24</sup> When the SWNTs are positively charged, Coulomb repulsion and van der Waals force exist simultaneously. These positive charges will distribute at the tips and outer surfaces of SWNTs because of the repulsive force of these charges.<sup>27</sup> At equilibrium, the resultant electric field will be perpendicular to the surface and the electrostatic potential is equal for every part of these SWNTs. With the electrostatic potential increased, the repulsive force  $f_c$  or the repulsive Coulomb energy  $E_c$  increased accordingly. Once the Rayleigh instability limit is reached, van der Waals force will be balanced by the Coulomb repulsion. At this point, increasing of charges will cause the occurrence of Coulomb explosion and the separation of SWNTs happens (Figure 4b). According to this model and analysis, we assume that SWNTs carry uniform linear charge density,  $q$ , as shown in Figure 4c. The electrostatic potential produced by these charges at a distance  $r_0$  can be calculated with the following equation

$$U = \int_{r_0}^{\infty} E dr = \int_{r_0}^{\infty} \frac{ql}{2\pi\epsilon_0 r \sqrt{r^2 + l^2}} dr = -\frac{q}{2\pi\epsilon_0} \ln\left(\sqrt{\left(\frac{l}{r_0}\right)^2 + 1} - \frac{l}{r_0}\right) \quad (2)$$

where  $\epsilon_0$  is vacuum permittivity, and  $2l$  the length of SWNTs. The repulsive Coulomb energy  $E_c$  can be expressed as

$$E_c = \frac{1}{2}QU \quad (3)$$

where  $Q$  is the total charges on the SWNTs ( $Q = 2lq$ ). Combining eqs 1, 2, and 3 at Rayleigh instability limit, the potential applied on SWNTs can be obtained with the following equation:

$$U = \sqrt{\frac{-2E_s \ln\left(\sqrt{\left(\frac{l}{r_0}\right)^2 + 1} - \frac{l}{r_0}\right)}{\pi\epsilon_0 l}} \quad (4)$$

According to the model (Figure 4 and Supporting Information),  $r_0$  has a typical value of 3.54 nm. Assuming the length  $2l$  of SWNTs to be  $\sim 2 \mu\text{m}$ , the potential needed for Coulomb explosion is estimated to be 7.2 V. Although this value is a little less than that used in our experiment, considering the difference of the assumed model with the actual bundle of SWNTs (such as the charge density is not strictly uniform along the whole length of SWNTs bundle and the effect of the charges at the tips of SWNTs bundle is neglected), the estimation is still quite consistent with our proposed mechanism of Coulomb explosion in this technique of separation SWNTs in a bundle.

According to eq 1 and 3, the linear charge density  $q$  at the point of the Coulomb explosion can be deduced with the following equation,  $q = 2E_s/lU$ , where  $l$  is the half-length of SWNTs, and  $U$  the voltage at the point of the Coulomb explosion. Then  $q$  is estimated to be  $\sim 0.14 e/\text{nm}$ . Considering

individual SWNT with a diameter of 1.6 nm,<sup>24,25</sup> the charge per carbon atom is roughly  $0.9 \times 10^{-2} e$  (Supporting Information), which is comparable to the reported value ( $6.7 \times 10^{-2} e$ ) found in an electrospinning procedure.<sup>28</sup>

Another quite interesting feature is that the separation of SWNTs is usually observed at the tip of the SWNT bundle that is far from SWNT rope. The reason may be the other tip of SWNTs is more tightly attached to the SWNTs rope. These features are similar to the case of a human hair when it is electrically charged. As illustrated in Figure 4d, the hairs separate from each other and extend radially from the head. The similarity of these two phenomena further confirms our proposed mechanism of Coulomb explosion based on electrostatic charging.

We also characterize the SWNT rope, bundles, and nanotrees with micro-Raman spectroscopy (Renishaw in via Raman spectroscope) by using a 632.8 nm He-Ne laser with a laser spot of  $\sim 1 \mu\text{m}$ . Figure 5 shows the radial breathing modes (RBMs) and G band of the SWNTs from sites “a–d” in Figure 1. Interestingly, both the RBMs and G band of these sites display significant differences from each other. According to the relationship between diameter ( $d$ ) of SWNTs and frequency ( $\omega_{\text{RBM}}$ ) ( $\omega_{\text{RBM}} = 224/d + 10$ ),<sup>29</sup> we can roughly estimate the diameter distribution of SWNTs in the SWNTs rope (site a), which ranges from 1.0 to 1.8 nm, agreeing well with our results measured by AFM.<sup>24,25</sup> From sites a–d, the number of RBM peaks detected in the Raman spectra decrease gradually, indicating the diameter of SWNT bundles becomes smaller and hence the number of SWNTs in each bundle becomes less. Meanwhile, the G band also shows quite different features, which exhibit more detailed components and become more complicated. This could be attributed to charge transfer phenomenon,<sup>30</sup> as well as the strain and deformation occurred during Coulomb explosion

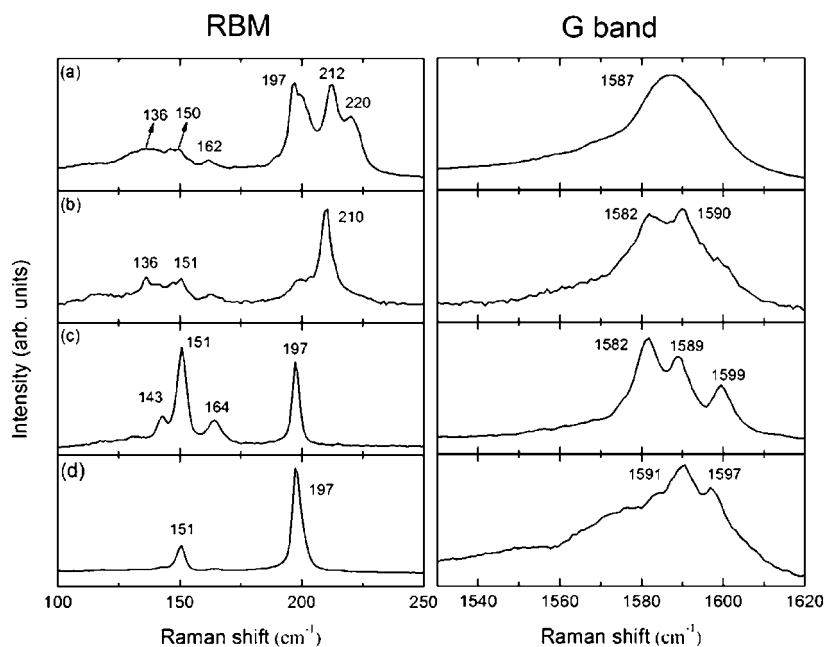


**Figure 5.** Raman spectra of SWNTs collected at different sites of those marked in Figure 1. Panels a–d correspond to sites a–d marked in Figure 1, respectively.

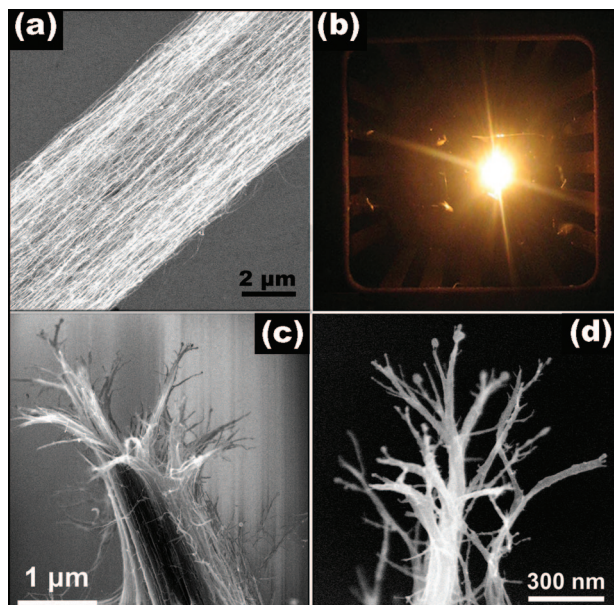


**Figure 6.** (a) SEM image of the SWNT bundles used for electrical breaking-down experiment. (b) Luminous SWNT bundle in vacuum. (c,d) SEM images of the typical nanotrees of SWNTs formed at the breaking points of SWNTs bundle.

process.<sup>29,31</sup> Finally, it should be noted that we did not observe successfully resonant RBM signals of individual SWNTs at the terminals of the “nanotree”, although weak G bands of individual SWNTs have been observed.

Interestingly, we also observed similar morphologies of SWNTs at the breaking points by electrical heating in vacuum. In our experiment, a two-terminal SWNT device was heated with a DC bias around 10 V in a vacuum of  $1 \times 10^{-3}$  Pa. Figure 6a shows the SEM image of the as-grown SWNT bundle used in our experiment. After heating about 10 min, the SWNT bundle illuminated (Figure 6b) and finally broke down caused by Joule heating. Figure 6c, d are the low and high magnification SEM images of the SWNTs at the breaking points. It can be seen that the SWNTs have a tendency to separate from each other, which is very similar to a recent report in MWNTs by Wei et al. and could be explained as a high local electric field and low vacuum at the instant of breakdown.<sup>32</sup> In addition, the tips of the SWNTs are compacted tightly and take the spherical shape. This is due to the surface tension produced by the melted carbon and/or catalyst at the breakdown instant.<sup>32</sup> This mechanism is different from what we demonstrate and propose in this letter. Because of the large diameter of SWNTs bundles at that breaking point (typically 40~60 nm), it is difficult to get smaller bundles or individual SWNT by this technique.

In conclusion, a simple and effective method based on Coulomb effect for separating SWNTs has been developed. With this method, we can easily obtain smaller bundles with uniform diameter as well as some individual SWNTs. The separated SWNTs are radially distributed at the end of the original bundle and finally form a nanotree. The formation mechanism is proposed to be Coulomb explosion. This approach provides possible applications for studies of

individual SWNTs devices and SWNT-based multiterminal devices. Moreover, this method may potentially be extended to the separation and the synthesis of other nanomaterials by introducing Rayleigh instability.

**Acknowledgment.** This work is supported by the “100 Talents Program” of Chinese Academy of Sciences, “973” Program of Ministry of Science and Technology (2006CB932402), and National Science Foundation of China (Grant 50702015, 10574034, 10774032).

**Supporting Information Available:** This material is available free of charge via the Internet at <http://pubs.acs.org>.

## References

- (1) Iijima, S.; Ichigashi, T. *Nature (London)* **1993**, *363*, 603.
- (2) Dresselhaus, M. S.; Dresselhaus, G.; Eklund, P. *Science of fullerenes and carbon nanotubes*; Academic Press: New York, 1996.
- (3) Hamada, N.; Sawada, S.; Oshiyama, A. *Phys. Rev. Lett.* **1992**, *68*, 1579.
- (4) Wildàer, J. W. G.; Venema, L. C.; Rinzler, A. G.; Smalley, R. E.; Dekker, C. *Nature (London)* **1998**, *391*, 59.
- (5) Odom, T. W.; Huang, J.-L.; Kim, P.; Lieber, C. M. *Nature (London)* **1998**, *391*, 62.
- (6) Girifalco, L. A.; Hodak, M.; Lee, R. S. *Phys Rev B* **2000**, *62*, 13104.
- (7) O’Connell, M. J.; Bachilo, S. M.; Huffman, C. B.; Moore, V. C.; Strano, M. S.; Haroz, E. H.; Rialon, K. L.; Boul, P. J.; Noon, W. H.; Kittrell, C.; Ma, J.; Hauge, R. H.; Weisman, R. B.; Smalley, R. E. *Science* **2002**, *297*, 593.
- (8) Rochefort, A.; Salahub, D. R.; Avouris, P. *Chem. Phys. Lett.* **1998**, *297*, 45.
- (9) Liu, J.; Rinzler, A. G.; Dai, H.; Hafner, J. H.; Bradley, R. K.; Boul, P. J.; Lu, A.; Iverson, T.; Shelimov, K.; Huffman, C. B.; Rodriguez-Macias, F.; Shon, Y.-S.; Lee, T. R.; Colbert, D. T.; Smalley, R. E. *Science* **1998**, *280*, 1253.
- (10) Chen, J.; Hamon, M. A.; Hu, H.; Chen, Y.; Rao, A. M.; Eklund, P. C.; Haddon, R. C. *Science* **1998**, *282*, 95.
- (11) Dalton, A. B.; Stephan, C.; Coleman, J. N.; McCarthy, B.; Ajayan, P. M.; Lefrant, S.; Bernier, P.; Blau, W. J.; Byrne, H. J. *J. Phys. Chem. B* **2000**, *104*, 10012.
- (12) Doorn, S. K.; Fields, R. E.; Hu, H.; Hamon, M. A.; Haddon, R. C.; Selegue, J. P.; Majidi, V. *J. Am. Chem. Soc.* **2002**, *124*, 3169.
- (13) Heller, D. A.; Mayrhofer, R. M.; Baik, S.; Grinkova, Y. V.; Usrey, M. L.; Strano, M. S. *J. Am. Chem. Soc.* **2004**, *126*, 14567.
- (14) Duesberg, G. S.; Blau, W.; Byrne, H. J.; Muster, J.; Burghard, M.; Roth, S. *Synth. Met.* **1999**, *103*, 2484.
- (15) Chattopadhyay, D.; Lastella, S.; Kim, S.; Papadimitrakopoulos, F. *J. Am. Chem. Soc.* **2002**, *124*, 728.
- (16) Niyogi, S.; Hu, H.; Hamon, M. A.; Bhowmik, P.; Zhao, B.; Rozenzhak, S. M.; Chen, J.; Itkis, M. E.; Meier, M. S.; Haddon, R. C. *J. Am. Chem. Soc.* **2001**, *123*, 733.
- (17) Farkas, E.; Anderson, M. E.; Chen, Z.; Rinzler, A. G. *Chem. Phys. Lett.* **2002**, *363*, 111.
- (18) Kamaras, K.; Itkis, M. E.; Hu, H.; Zhao, B.; Haddon, R. C. *Science* **2003**, *301*, 1501.
- (19) Hu, H.; Zhao, B.; Hamon, M. A.; Kamaras, K.; Itkis, M. E.; Haddon, R. C. *J. Am. Chem. Soc.* **2003**, *125*, 14893.
- (20) Shin, H.-J.; Kim, S. M.; Yoon, S.-M.; Benayad, A.; Kim, K. K.; Kim, S. J.; Park, H. K.; Choi, J.-Y.; Lee, Y. H. *J. Am. Chem. Soc.* **2008**, *130*, 2062.
- (21) Lord Rayleigh, *Philos. Mag.* **1882**, *14*, 184.
- (22) Han, Y.; Zhu, J. Y.; Liu, F.; Li, S.-C.; Jia, J.-F.; Zhang, Y.-F.; Xue, Q.-K. *Phys. Rev. Lett.* **2004**, *93*, 106102.
- (23) Zhang, Z. X.; Sun, L. F.; Zhao, Y. C.; Liu, Z.; Liu, D. F.; Cao, L.; Zou, B. S.; Zhou, W. Y.; Gu, C. Z.; Xie, S. S. *Nano Lett.* **2008**, *8*, 652.
- (24) Liu, G. T.; Zhao, Y. C.; Deng, K.; Liu, Z.; Chu, W. G.; Chen, J. R.; Yang, Y. L.; Zheng, K. H.; Huang, H. B.; Ma, W. J.; Song, L.; Yang, H. F.; Gu, C. Z.; Rao, G. H.; Wang, C.; Xie, S. S.; Sun, L. F. *Nano Lett.* **2008**, *8*, 1071.

- (25) Zhao, Y. C.; Song, L.; Deng, K.; Liu, Z.; Zhang, Z. X.; Yang, Y. L.; Wang, C.; Yang, H. F.; Jin, A. Z.; Luo, Q.; Gu, C. Z.; Xie, S. S.; Sun, L. F. *Adv. Mater.* **2008**, *20*, 1772.
- (26) Last, I.; Levy, Y.; Jortner, J. *Proc. Natl. Acad. Sci. U.S.A.* **2002**, *99*, 9107.
- (27) Guan, L. H.; Shi, Z. J.; Gu, Z. N. *Carbon* **2005**, *43*, 1101.
- (28) Gao, J.; Yu, A.; Itkis, M. E.; Bekyarova, E.; Zhao, B.; Niyogi, S.; Haddon, R. C. *J. Am. Chem. Soc.* **2004**, *126*, 16698.
- (29) Rao, A. M.; Chen, J.; Richter, E.; Schlecht, U.; Eklund, P. C.; Haddon, R. C.; Venkateswaran, U. D.; Kwon, Y. K.; Tománek, D. *Phys. Rev. Lett.* **2001**, *86*, 3895.
- (30) Dresselhaus, M. S.; Dresselhaus, G.; Saito, R.; Jorio, A. *Phys Rep* **2005**, *409*, 47.
- (31) Song, L.; Ci, L.; Lv, L.; Zhou, Z. P.; Yan, X. Q.; Liu, D. F.; Yuan, H. J.; Gao, Y.; Wang, J. X.; Liu, L. F.; Zhao, X. W.; Zhang, Z. X.; Dou, X. Y.; Zhou, W. Y.; Wang, G.; Wang, C. Y.; Xie, S. S. *Adv. Mater.* **2006**, *16*, 1529.
- (32) Wei, Y.; Jiang, K.; Liu, L.; Chen, Z.; Fan, S. S. *Nano Lett.* **2007**, *7*, 3792.

NL802827M